From Z-Machines to ALMA: (Sub)millimeter Spectroscopy of Galaxies
ASP Conference Series, Vol. TBD, 2006
A. J. Baker, J. Glenn, A. I. Harris, J. G. Mangum, and M. S. Yun, eds.

The Zpectrometer: an ultra-wideband spectrometer for the Green Bank Telescope

A.I. Harris[1], A.J. Baker[1,2,3], P.R. Jewell[2], K.P. Rauch[1], S.G. Zonak[1], K. O'Neil[2], A.L. Shelton[2], R.D. Norrod[2], J. Ray,[2] and G. Watts[2]

[1]*Department of Astronomy, University of Maryland, College Park, MD 20742;*
[2]*National Radio Astronomy Observatory, P.O. Box 2, Green Bank, WV, 24944*
[3]*National Radio Astronomy Observatory Jansky Fellow*

Abstract. We describe the *Zpectrometer*, an ultra-wideband radio spectrometer for the Green Bank Telescope (GBT). Observations with this instrument will be important for understanding the star formation, metal production, and structure formation histories of the Universe. The *Zpectrometer* covers the full 13.5 GHz-wide Ka-band with a set of analog lag correlation spectrometers in a multi-channel correlation radiometer architecture. Its bandwidth and stability, combined with the GBT's collecting area, enable sensitive and efficient spectral searches for molecules in high redshift galaxies. The instrument is optimized for observations of low-excitation spectral lines from the carbon monoxide (CO) molecule at redshifts of $1.88 \leq z \leq 3.43$ and $4.76 \leq z \leq 7.87$.

All high-redshift radio molecular detections to date have started from optical redshifts. *Zpectrometer*'s wide bandwidth bypasses this selection effect and enables it to detect new classes of sources. In addition to finding precise redshifts, its approximately 150 km s^{-1} resolution spectra probe kinematical signs of interaction and enable dynamical mass estimates. Because both cold and warm gas emit low-J lines these observations place critical constraints on radiative transfer models of physical conditions.

1. Introduction

The *Zpectrometer*'s main purpose is to study star and galaxy formation in the early Universe. The histories of these processes are coupled with the evolution of large-scale structure and the formation of metals, and are thus of fundamental cosmological interest. The *Zpectrometer* is a heterodyne spectrometer that will cover the entire Ka-band (26.5-40 GHz) at the 100-meter Robert C. Byrd Green Bank Telescope (GBT). This ultra-wideband spectrometer is a spectral bridge between observations with continuum cameras that search for luminous dusty galaxies at high redshift and line observations with radio and millimeter-wave interferometers. It is optimized for velocity-resolved spectroscopy of cold and warm molecular gas to explore the physical state and mass of young massive galaxies. Line-resolved spectroscopy will also constrain dynamical masses the gas for mass estimates and identify kinematic signatures of interactions.

Of the instruments described this *Proceedings*, the *Zpectrometer* covers the lowest frequencies, corresponding to rest-frame millimeter-wave spectral lines

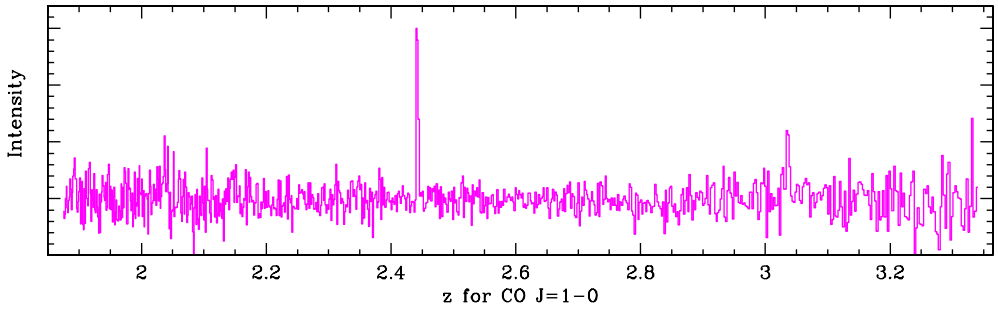

Figure 1. Simulated *Zpectrometer* spectrum: the full Ka-band in 825 channels with CO $J = 1$–0 lines at $z = 2.34$ (34.5 GHz) and 3.03 (28.5 GHz). The noise in the simulation is scaled by the GBT's measured receiver temperature and telescope aperture efficiency.

from low-excitation molecular transitions near $z \sim 2$–3. With nearly 1000 spectral channels across the band, its spectral resolution is sufficient to extract lineshape information.

By covering the entire Ka-band, the *Zpectrometer* is able to make velocity-unbiased searches for low-excitation spectral lines of carbon monoxide (CO) molecules to determine precise redshifts of young galaxies at cosmological distances. Figure 1 is a simulated *Zpectrometer* spectrum over its full CO $J = 1$–0 $1.88 \leq z \leq 3.43$ (lookback times of 10.1–11.8 Gyr) band with a spectral resolution of approximately 150 km s^{-1}. The same observed-frame frequencies also correspond to the $J = 2$–1 transition at $4.76 \leq z \leq 7.87$ (from 12.4–13.0 Gyr ago, just 700 Myr after the Big Bang), covering the era of final reionization.

A combination of HEMT amplifier receivers and wideband analog lag spectrometers makes it possible to search the Ka-band's entire 41% fractional bandwidth (instantaneous bandwidth divided by average frequency) for spectral lines. A correlation radiometer architecture, similar to the continuum radiometers on the WMAP satellite, will help provide excellent baseline stability.

The GBT is uniquely well suited for studies of the early Universe. It has an off-axis reflector with an unblocked 100-meter equivalent aperture. The GBT's active surface already provides excellent performance in the Ka-band, and the surface will improve as upgrades continue for telescope operation at 115 GHz. This combination of geometrical area and a precise surface gives the GBT an enormous collecting area; at centimeter wavelengths the GBT has an equivalent collecting area larger than the 27-antenna Expanded Very Large Array, EVLA. Combined with state-of-the-art receivers, the GBT provides extraordinary sensitivity for observations of point sources.

2. Star and galaxy formation in the early Universe

2.1. Targets

Other papers in this *Proceedings* discuss observational evidence that the cosmic star formation rate peaked somewhere between z of 2 and 5. Current wisdom holds that $z \sim 2$–3 defines the epoch when many of the long-lived stars in the

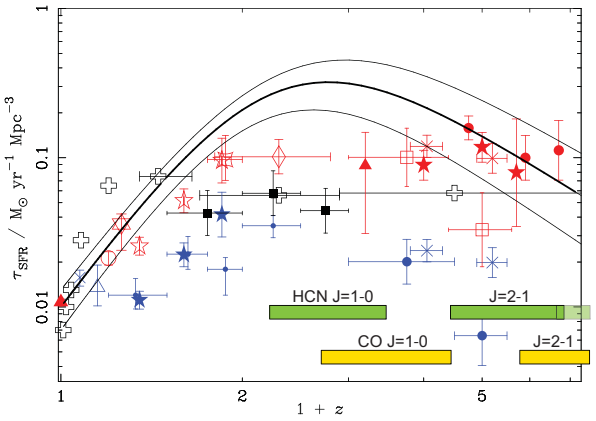

Figure 2. Star formation rate density versus redshift z, updated from Blain et al. 2002 (Blain 2004, priv. comm.). Points with error bars are derived from rest-frame UV observations and show the considerable uncertainty in the star formation rate density. The heavy solid line is the best-fit evolutionary model derived from submillimeter and far-IR observations alone; lighter lines show model error limits. Bars toward the bottom of the panel show Ka-band coverage for low-J CO and HCN lines.

Universe formed, the assembly of massive galaxies by mergers was especially vigorous, supermassive black holes formed, and QSO activity increased dramatically. The details of this picture are far from settled, however. An important constraint on models of structure formation is a census of massive galaxies as a function of redshift. Rest-frame millimeter-wave molecular emission escapes easily through the dust that hides young massive galaxies in optical images, with velocity-resolved spectroscopy providing dynamical mass estimates independent of the uncertainties in dust or molecular emissivity per unit mass.

Although of order 30 galaxies and quasars have been detected in CO at redshifts $1.4 < z < 6.4$ (summaries in e.g. Hainline et al. 2004; Greve et al. 2005; Solomon and vanden Bout 2005), it is important to recognize that *all of these molecular detections to date have started from optical redshifts.* The need for optical detection complicates and biases searching for and exploring the state of molecular gas in young galaxies. Initial *Zpectrometer* molecular line observations will have fewer and different selection effects: it will make an unbiased search for molecular emission over a very wide band.

An obvious search strategy for dusty submillimeter galaxies (SMGs) is to start with source positions from the many sensitive sub-mm and mm-wave continuum cameras that have been built to observe the high-z universe. All of the ground-based cameras provide source position accuracies well matched to the GBT's 23″–15″ Ka-band beam, eliminating the need to search within the continuum camera beams.

The *Zpectrometer* will also sample populations other than the dusty galaxies selected in the submillimeter. This is important for exploring the connections between the SMGs and other populations. It will be sensitive to galaxies with warmer dust that the Spitzer Space Telescope (SST) detects but that 850 μm continuum observations miss (e.g. Houck et al. 2005; Yan et al. 2005). More

targets will emerge from other deep far-IR through X-ray imaging programs (e.g. Herschel-SPIRE, Chandra, Newton-XMM...) and steep-spectrum radio galaxy searches (e.g. Reuland et al. 2004).

2.2. The role of spectroscopy

Although the *Zpectrometer*'s band is very wide, the 115 GHz spacing between CO transitions is too large for more than one line to appear in the the band until $z \sim 10$. Emission from the HCN molecule, a tracer of dense gas associated with star formation (Gao and Solomon 2004), will be detectable from bright sources and will provide redshift confirmation over the redshift ranges $z = 1.88$–2.41 where the CO and HCN $J = 1$–0 lines both fall in the band (Fig. 2).

Millimeter-wave interferometers can quickly follow most or all of the *Zpectrometer* detections with observations of higher-J CO lines. These will provide unambiguous redshifts from detection of two or more lines, constrain physical conditions with line ratios, and generate detailed spatial maps and spectra. High-resolution imaging is necessary to identify sources that are gravitationally lensed and to build models for the gravitational magnification. Interferometers have relatively narrow bandwidths at present, however, and must start with precise redshifts. Shifts between optical and radio lines can be large in radio galaxies and may be the reason that at least some of the narrowband CO searches in dusty galaxies based on optical redshifts have failed.

2.3. Cold gas and low-J lines

Observations in the Ka-band contain the lowest-excitation transitions of the abundant carbon monoxide molecule from sources at $z \sim 2$–3. Lines from low-J states probe relatively cold or low density gas as well as the warm and dense gas that rest-frame submillimeter emission preferentially traces. CO $J = 1$–0 luminosity is therefore taken as a proxy for molecular gas mass. Almost all of the high-z CO detections to date have been at millimeter wavelengths because of the lack of suitable cm-wave instrumentation.

Measurements of the low excitation lines are necessary for modeling the realistic situation of a source with more than one temperature component. Figure 3 is a two-component decomposition of a $z = 3$ starburst based on the conditions in the starburst galaxy M82. Constraining the relative amounts of cold and warm gas requires low-J measurements sensitive to cool gas; without this information, the properties of even the warm gas component alone are uncertain within orders of magnitude. The importance of cool components is obscured in plots of flux vs. frequency because of the frequency squared scaling between brightness temperature and flux. Full modeling is needed to understand the amount of gas in each component.

2.4. Typical integration times

Extrapolating from detections of the current sample of dusty galaxies and quasars permits estimates for line fluxes and integration times. Many of these sources have mm-wave line fluxes of a few mJy. With a representative set of telescope parameters and source zenith angles we derive a system temperature of 100 K and an rms fluctuation of 0.18 mK after 10 hours of integration in a single 17 MHz channel. With the GBT's conversion of 1.1 K/Jy (350 μm rms surface,

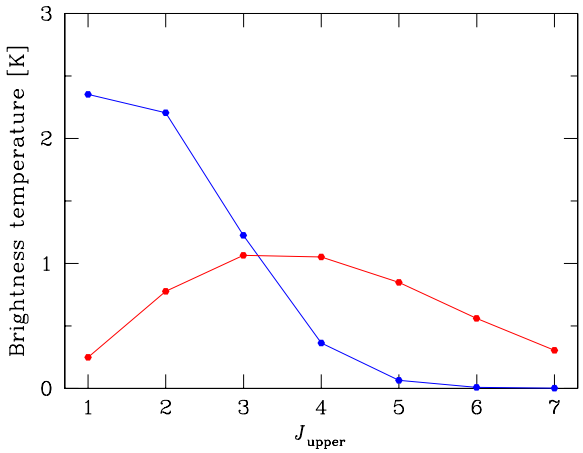

Figure 3. Two-component radiative transfer model of a $z = 3$ starburst nucleus patterned on conditions in M82. A 23 K component has peak emission at low rotational quantum numbers J, while a 208 K component is optically thin in the low-J transitions and peaks near $J \sim 3$–4. Both components in this model have equal mass but different filling factors within the beam.

33 GHz), this corresponds to 0.16 mJy rms. This integration time is feasible for some tens of sources per year. Line flux increases with frequency for a thermalized source, and cosmological dimming is favorable at high redshift, so observations of higher-J lines are quite possible at even higher redshifts.

3. Technical aspects

3.1. Correlation radiometry

A key element of the *Zpectrometer* is its use of correlation techniques in the receiving system. Cross-correlating brings the stability advantages of a continuum correlation radiometer to spectroscopy. Spectroscopy with correlation techniques on a single-dish telescope is unusual in radio astronomy. A number of groups investigated single-dish correlation receivers during the 1960s as an alternative to the standard Dicke-switched radiometer, but the cost of building two receiver chains and cross-correlators limited their use to special cases such as centimeter-wave radio continuum studies, a rapid-response millimeter-wave radiometer (Haslam et al. 1974; Predmore et al. 1985), and, more recently, radiometers for observations of the Cosmic Microwave Background (e.g. WMAP; Jarosik et al. 2003). Analysis and laboratory tests show that this method will work very well for spectroscopy as well (Harris 2005). Correlation radiometry with the WASP2 analog lag correlators (Harris and Zmuidzinas 2001) has several practical advantages past the essential characteristic of excellent stability. First, a correlation receiver's two beams double the observing time efficiency compared with a conventional single-pixel receiver. Next, the two beams need only one cross-correlating analog lag spectrometer for a dual-beam receiving system, a significant savings in cost and complexity. Finally, analog correlators do not

have the quantization noise penalty that can cost digital systems up to a factor of ~ 1.2 in signal to noise ratio.

Correlation detection is very stable because it makes an instantaneous differential power measurement. This greatly suppresses nonideal noise terms compared with conventional total power measurements. Consider first a total power radiometer with gain G, input source voltage v_{sou}, and system noise voltage v_n. Its detector output voltage v_{out} is proportional to $G\langle v^2_{detector}\rangle$, or $v_{out} \propto G\left(\langle v^2_{sou}\rangle + \langle v^2_n\rangle\right)$, plus a cross term that averages away with time as $1/\sqrt{B\tau}$. Spatial chopping and differencing between source and reference positions on the sky largely eliminates the relatively large noise signal $\langle v^2_n\rangle$, but even tiny fluctuations in system gain G or noise power at the chop frequency can produce signals much larger than the weak source signal, $\delta\left(G\langle v^2_n\rangle\right) \gg \langle v^2_s\rangle$.

Cross-correlating radiometers have a hybrid circuit that combines voltages from the source and reference positions, v_s and v_r, with different but known phase shifts before amplification (Fig. 4). Cross-correlating the signals from the two amplifiers with the proper phase extracts the power difference between the source and reference positions, $v_{out} \propto G(\langle v^2_{sou}\rangle - \langle v^2_{ref}\rangle)$. Uncorrelated terms, including those from amplifier gain fluctuations, average away with time as $1/\sqrt{B\tau}$. Gain fluctuations have no large noise term to amplify, greatly reducing the excess noise across the spectrum. A full analysis (Harris 2005) shows that amplitude and phase imbalance reduce the signal but do not add correlated noise terms to the output.

Mathematics aside, a simple way to understand the technique is as a complement to the two-element spatial interferometer, where the correlated signal from two different antennas and receivers contains only information on the signal in common: that of the source. A single-dish correlation radiometer arranges the signal paths with as much commonality as possible; the only signals that are separate are the two from the signal and reference positions in the focal plane. The result, rather than the interferometer's detection of *correlated* signal in the aperture plane, is the difference of the *uncorrelated* power between two points in the focal plane.

3.2. Zpectrometer hardware

Figure 4 is a top-level overview of the spectrometer system. NRAO is commissioning the Ka-band (26.5–40 GHz) correlation radiometer that we will use for the spectrometer's front-end. This radiometer was designed with an architecture similar to the WMAP radiometers (Jarosik et al. 2003) for sensitive radio continuum measurements. After downconversion within the front-end into the 4–18 GHz band, an IF processor splits the signal into four 4–8 GHz band inputs for the cross-correlating spectrometers. A modest number of sub-bands allows compensation for slow changes in receiver and transmission system band flatness without introducing too many edge effects. Eight WASP2 analog lag correlation spectrometers (Harris and Zmuidzinas 2001), each with 3.7 GHz bandwidth and 128 lags, produce the spectrum of the receiver band.

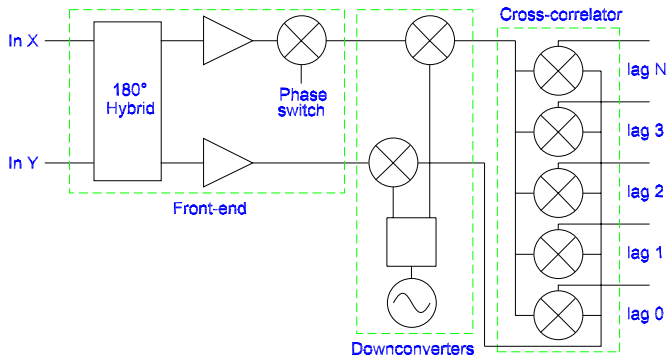

Figure 4. Top-level block diagram of the *Zpectrometer* system showing the Ka-band front-end, channelizing downconverter, and cross-correlator. See Fig. 5 for more detail on the correlator.

An analog lag correlator uses analog delays and multiplication to estimate the cross-correlation function $R_{XY}(\tau)$ as a function of lag τ:

$$R_{XY}(\tau) = \lim_{T\to\infty} \frac{1}{2T} \int_{-T}^{T} v_X(t) \cdot v_Y(t+\tau)\, \mathrm{d}t \; . \tag{1}$$

A Fourier transform of the cross-correlation function yields the power density cross-spectrum, which for the *Zpectrometer* is the power difference between the source and reference positions.

Figure 5 is a schematic diagram showing the correlator circuit board layout. The boards carry transmission lines that provide the time delays τ between multiplier inputs, transistor multipliers that form the product of the two input voltages $v_A(t)$ and $v_B(t+\tau)$, and low-frequency electronics to integrate the multiplier output to provide the time average. Multiplier spacing sets the spectrometer's maximum bandwidth through the Nyquist theorem; increasing the total lag time by adding multipliers to the ladder provides proportionally higher spectral resolution. The analog multipliers are commercial monolithic microwave integrated circuit (MMIC) transistor mixers with fast transistors in the same classical Gilbert multiplier core circuit (Gilbert 1968) that is in audio-frequency multiplier chips. Direct multiplication at the signal frequency means that only the low-frequency product term is digitized, saving considerable complexity and power dissipation.

Stability is a paramount concern for extragalactic spectrometers. WASP2's electronics have proved suitable for long integration times. Offset drift is usually the dominant problem for analog systems, but is largely removed by the layers of internal phase switching within WASP2. Allan variance characterization of spectrometer stability shows white noise to times beyond 100 seconds for the high lags, which should be representative of all lags in cross-correlation mode. This timescale is well within the timescale for efficient beam exchange at the GBT.

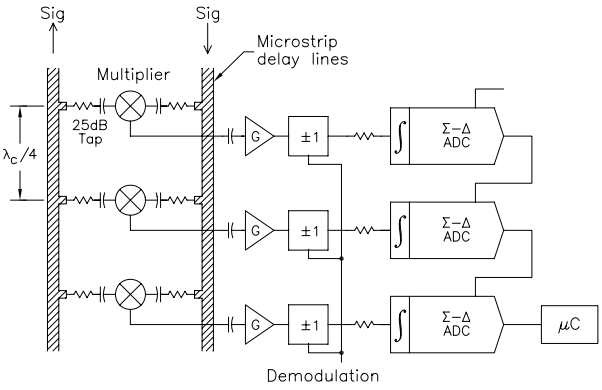

Figure 5. Schematic view showing a section of the "ladder" of multipliers within WASP2 and the low-frequency signal processing electronics. Sections of microstripline transmission line provide propagation-time delays between fast transistor multipliers.

3.3. Correlator configurations

Table 1 shows a number of possible correlator configurations that could cover different bands in different ways. The *Zpectrometer* correlator contains a total of 1024 lags that may be distributed in 128 lag subsets, each subset covering 3.5 GHz. The initial configuration for Ka-band, shown in bold, is 4 sub-bands of 256 lags. This covers as much bandwidth as possible and requires no tuning between the front-end and the correlator package.

Bandwidth GHz	Resolution MHz	Polarizations	Number of sub-bands	Lags per sub-band
28	32.8	1	8	128
14	**16.4**	**1**	**4**	**256**
7	8.2	1	2	512
7	16.4	2	2	256
3.5	16.4	2	1	512

Table 1. Some possible correlator configurations. Switching between configurations requires some modification of the downconversion electronics and some internal cables. Boldface denotes the *Zpectrometer*'s initial configuration.

In this initial configuration, the *Zpectrometer* will cover the entire Ka-band with spectral resolution of about 150 km s^{-1}. This is sufficient for characterizing the dynamics of high-redshift galaxies. Hainline et al. (2004) summarize 27 published CO detections from $z > 1.4$ galaxies, finding a median FWHM velocity width of 380 km s^{-1} and a range from 170 to 840 km s^{-1}, values confirmed by later observations (Greve et al. 2005; Tacconi et al. 2006). WASP2 configured for 256 lags matches this very well. Figure 6a is a 128-lag WASP2 spectrum of the 230 GHz CO $J = 2$–1 line from the starburst nuclear ring in the Seyfert galaxy NGC1068, which has a width of about 300 km s^{-1}. This spectrum obtained in one of four contiguous sub-bands obtained WASP2 correlators connected to the wideband 200–300 GHz receiver at the Caltech Submillimeter Observatory

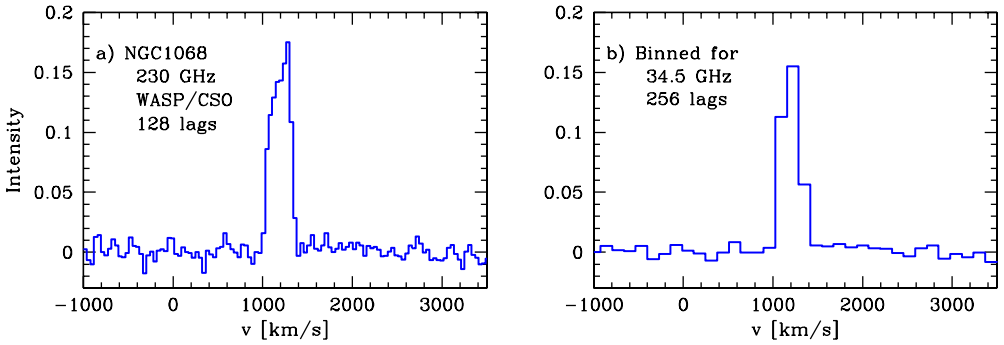

Figure 6. Measured and simulated signals from the WASP spectrometers. a) Measured CO $J = 2$–1 line at the CSO with 128 lag autocorrelator mode; b) Same spectrum binned to show resolution at 34.5 GHz with 256 lags.

in August 2003. No corrections have been applied to the spectral baseline. Figure 6b is the same spectrum binned to simulate an observation of the same source in the CO $J = 1$–0 line at $z = 2.3$ (34.5 GHz) with a 256-lag WASP2.

Connecting the *Zpectrometer* back-end hardware to other GBT front-ends can provide wideband spectroscopy at all values of z. Obvious extensions are to reconfigure for autocorrelation with the K-band (18-26.5 GHz) or Q-band (40-50 GHz) front-ends. These are conventional total-power receivers, so the advantages of correlation techniques would be lost. An additional downconverter system and minor internal recabling would permit coverage of the entire 28 GHz W-band (3 mm) HEMT amplifier bands with 33 MHz resolution and benefit from the GBT's W-band front-end's correlation architecture.

3.4. Data acquisition and analysis

Each pair of correlators shares an internal microcontroller that handles all real-time data acquisition and accumulates the correlator digital output for a sub-scan integration time, typically of a few minutes. An Ethernet connection transmits lag data from the microcontroller to one of the GBT's computers for pipeline reduction that converts from lag to spectral domain, calibrates amplitude and frequency scales, and writes a file for incorporation into the GBT data system. The observatory sets parameters and otherwise controls the *Zpectrometer* within a standard GBT software manager task that serves as a wrapper for the WASP2 code developed for stand-alone operation.

Finding lines within a spectrum of over 40% bandwidth is unlike previous radio spectroscopy. We are developing analysis tools that use the time series as well as the average spectrum to estimate fluctuations for each spectral channel; see Zonak, Baker, and Harris in this *Proceedings* for further details.

4. Timeline and operation

Fabrication began in March 2005 with a target for first tests in the winter of 2006/2007 and science observations the following winter. The *Zpectrometer* is a collaboration between the University of Maryland (UMD) and the National Ra-

dio Astronomy Observatory (NRAO). Consistent with NRAO's policy on guest instruments, this system will be available for some shared-risk community proposals after early commissioning. The instrument will transition to facility-mode operation after winter 2007/2008.

Acknowledgments. The *Zpectrometer* is being constructed with National Science Foundation (NSF) grant AST-0503946 to the University of Maryland. The NRAO is operated for the NSF by Associated Universities, Inc., under a cooperative agreement.

References

C. M. Bradford, T. Nikola, G. J. Stacey, A. D. Bolatto, J. M. Jackson, M. L. Savage, J. A. Davidson, and S. J. Higdon. ApJ, 586: 891–901, 2003.
D. Downes and P. M. Solomon. ApJ, 507: 615–654, 1998.
Y. Gao and P. M. Solomon. ApJ, 606: 271–290, 2004.
B. Gilbert. IEEE J. Solid-State Circuits, 3: 365–373, 1968.
T. R. Greve et al. MNRAS, 359: 1165–1183, 2005.
L. J. Hainline, N. Z. Scoville, M. S. Yun, D. W. Hawkins, D. T. Frayer, and K. G. Isaak. ApJ, 609: 61–68, 2004.
A. I. Harris. Review of Scientific Instruments, 76: 4503–+, 2005.
A. I. Harris, J. Stutzki, U. U. Graf, A. P. G. Russell, R. Genzel, and R. E. Hills. ApJ, 382: L75–L79, 1991.
A. I. Harris and J. Zmuidzinas. Review of Scientific Instruments, 72: 1531–1538, 2001.
C.G.T. Haslam, W.E. Wilson, D.A. Graham, and G.C. Hunt. Astron. Astrophys. Suppl., 13: 359–394, 1974.
J. R. Houck et al. ApJ, 622: L105–L108, 2005.
N. Jarosik et al. Astrophys. J. Suppl. Ser., 145: 413–436, 2003.
M. L. Luhman, S. Satyapal, J. Fischer, M. G. Wolfire, E. Sturm, C. C. Dudley, D. Lutz, and R. Genzel. ApJ, 594: 758–775, 2003.
R. Q. Mao, C. Henkel, A. Schulz, M. Zielinsky, R. Mauersberger, H. Störzer, T. L. Wilson, and P. Gensheimer. A&A, 358: 433–450, 2000.
C.R. Predmore, N.R. Erickson, G.R. Huguenin, and P.F. Goldsmith. IEEE Trans. Microwave Theory Tech., MTT-33: 44–51, 1985.
M. Reuland, H. Röttgering, W. van Breugel, and C. De Breuck. MNRAS, 353: 377–390, 2004.
N. Z. Scoville, M. S. Yun, and P. M. Bryant. ApJ, 484: 702–+, 1997.
P.M. Solomon and P.A. vanden Bout. ARA&A, 43: 677-725, 2005.
L. J. Tacconi, R. Neri, S. C. Chapman, R. Genzel, I. Smail, R. J. Ivison, F. Bertoldi, A. Blain, P. Cox, T. Greve, and A. Omont. ApJ, 640: 228–240, March 2006.
J. S. Ward, J. Zmuidzinas, A. I. Harris, and K. G. Isaak. ApJ, 587: 171–185, 2003.
L. Yan et al. ApJ, 628: 604–610, 2005.